

# Distributional Random Forests: Heterogeneity Adjustment and Multivariate Distributional Regression

**Domagoj Ćevd\***  
ETH Zürich  
cevid@stat.math.ethz.ch

**Loris Michel\***  
ETH Zürich  
michel@stat.math.ethz.ch

**Nicolai Meinshausen**  
ETH Zürich  
meinshausen@stat.math.ethz.ch

**Peter Bühlmann**  
ETH Zürich  
peter.buehlmann@stat.math.ethz.ch

## Abstract

We propose an adaptation of the Random Forest algorithm to estimate the conditional distribution of a possibly multivariate response. We suggest a new splitting criterion based on the MMD two-sample test, which is suitable for detecting heterogeneity in multivariate distributions. The weights provided by the forest can be conveniently used as an input to other methods in order to locally solve various learning problems. The code is available as R-package `drf`.

## 1 Introduction

In practice one often encounters heterogeneous data: for example, data can be collected from several different sources or the data distribution might change with time. In the field of personalized medicine, one wants to determine the effect of a certain treatment depending on some patient characteristics such as age, race, gender, medical history, etc. Obviously, pooling heterogeneous data together can result in bad predictions. On the other hand, if one considers only the data on patients whose characteristics exactly match the target patient, one may end up with too few data points.

Let  $\mathbf{Y} = (Y_1, Y_2, \dots, Y_d) \in \mathbb{R}^d$  be a multivariate target variable, whose joint distribution may depend on a potentially large number of covariates  $\mathbf{X} = (X_1, X_2, \dots, X_p) \in \mathbb{R}^p$ . Throughout the paper, the vector values are denoted in bold. We aim to estimate the whole conditional distribution  $\mathbb{P}(\mathbf{Y} | \mathbf{X} = \mathbf{x}) = \mathbb{P}(\mathbf{Y} | X_1 = x_1, \dots, X_p = x_p)$ , where  $\mathbf{x} = (x_1, \dots, x_p)$  is an arbitrary point in  $\mathbb{R}^p$ . Given observed examples  $\{(\mathbf{x}_i, \mathbf{y}_i)\}_{1 \leq i \leq n}$ , the most straightforward way of doing it nonparametrically is by considering only the data points in some neighborhood  $\mathcal{N}_{\mathbf{x}}$  of the point of interest  $\mathbf{x}$ , e.g. by taking the nearest  $k$  neighbors. However, such methods typically suffer from the curse of dimensionality even when  $p$  is only moderately large: for a reasonably small neighborhood, such that the distribution  $\mathbb{P}(\mathbf{Y} | \mathbf{X} \in \mathcal{N}_{\mathbf{x}})$  is close to the distribution  $\mathbb{P}(\mathbf{Y} | \mathbf{X} = \mathbf{x})$ , the number of training data points contained in it will be very small, thus making the estimation of the conditional distribution  $\mathbb{P}(\mathbf{Y} | \mathbf{X} = \mathbf{x})$  difficult. The same phenomenon occurs with other methods which locally weight the training observations such as kernel methods [23], local MLE [8] or weighted regression [6] even for the simpler problem of estimating the conditional mean  $\mathbb{E}[\mathbf{Y} | \mathbf{X} = \mathbf{x}]$  when  $d = 1$ . For that reason, more importance needs to be given to the training data points  $(\mathbf{x}_i, \mathbf{y}_i)$  for which the response distribution  $\mathbb{P}(\mathbf{Y} | \mathbf{X} = \mathbf{x}_i)$  at point  $\mathbf{x}_i$  is similar to the target distribution  $\mathbb{P}(\mathbf{Y} | \mathbf{X} = \mathbf{x})$ , even if  $\mathbf{x}_i$  is not componentwise close to  $\mathbf{x}$  in the predictor space  $\mathcal{X}$ . Our procedure needs thus to be data-adaptive,

\*Alphabetical order, equal contribution of authors.

since one rarely knows a priori which covariates cause the heterogeneity of the response distribution  $\mathbb{P}(\mathbf{Y} \mid \mathbf{X} = \mathbf{x})$  and in which way.

In this paper, we propose the Distributional Random Forest (DRF) method which estimates the multivariate conditional distribution  $\mathbb{P}(\mathbf{Y} \mid \mathbf{X} = \mathbf{x})$  in a data-driven fashion. This is done by repeatedly dividing the data points in the spirit of the Random Forest algorithm [5]: at each step, we split the data points based on some feature  $X_i$  in such a way that the distribution of the responses  $\mathbf{Y}$  for which  $X_i \leq l$ , for some level  $l$ , is the most different compared to the responses with  $X_i > l$ . This partitions the data points so that the distribution of the responses in each resulting leaf is as homogeneous as possible. Repeating this many times with randomization induces a weighting function, described in detail in Section 2, which quantifies the relevance of each training data point for a given test point. The conditional distribution is then estimated by those weights.

Often one is not interested in the conditional distribution of  $Y$  per se, but instead in some functionals of it, such as, for example, the conditional quantiles [19], conditional correlations or joint conditional probability statements. These quantities can be easily estimated with DRF by computing them directly from the obtained weights. The weighting function might be even used for some more complicated objectives such as conditional independence testing [28], heterogeneous regression [17, 25] or semiparametric estimation by fitting a parametric model for  $Y$  after adjusting for  $X$  [4]. Furthermore, representing the conditional distribution via the weighting function can be helpful for applications in causality such as for determining the causal effects or as a way of implementing do-calculus [20] for finite samples. Therefore, DRF can be used as a two-step method, where in the first step one obtains the weighting function by building the trees and in the second step one uses the weights for further analysis.

**Related work and our contribution.** Using the Random Forest algorithm as an adaptive locally weighted estimator has been used for several applications, such as: survival analysis [13], quantile regression [19], parametric univariate conditional distribution estimation [14] and estimation of univariate parameters for which there is a local estimating equation of a certain form [2]. Our proposed methodology is not specific to a particular task and can be universally used in combination with many standard methods. There has not been much work in the literature on the forest-based methods handling multivariate responses. The existing approaches [16, 22] are based on averaging separate criteria for  $Y_1, \dots, Y_d$  (usually the standard CART criteria) and target only the conditional mean of the responses, a task which can also be solved by separate regression fits for each  $Y_i$ .

For better statistical performance, many forest-based methods use a splitting criterion tailored for their specific application, instead of relying on the standard CART criterion. For computational feasibility, one often needs to resort to approximating the splitting criterion [2]. We propose splitting based on a fast random approximation of the MMD two-sample test [10, 29], which is able to detect any change in distribution. However, our proposed methodology is very flexible and one could use any other two-sample test. We illustrate the versatility of DRF for many different learning problems.

## 2 Method description

In this section we describe the details of the implementation of the Distributional Random Forest (DRF) algorithm. We closely follow the implementations of the `grf` [2] and `ranger` [26] R-packages. All additional implementation details can be found in the supplementary material.

**Forest building.** The trees are grown as follows: For every parent node  $P$ , we determine how to best split it into two child nodes of the form  $C_L = \{X_j \leq l\}$  and  $C_R = \{X_j > l\}$ , where the predictor  $X_j$  is one of the randomly chosen splitting candidates and  $l$  denotes its level, such that we maximize certain (multivariate) two-sample test statistic

$$d(\{\mathbf{y}_i \mid \mathbf{x}_i \in C_L\}, \{\mathbf{y}_i \mid \mathbf{x}_i \in C_R\}). \quad (1)$$

It measures the difference of the distributions of the response  $Y$  in the two resulting child nodes. We therefore select the candidate predictor  $X_j$  which seems to affect the distribution of  $\mathbf{Y}$  the most. Intuitively, in this way we ensure that the distribution of the data points in every leaf of the resulting tree is as homogeneous as possible.

The constructed trees induce a weighting function, which is used to estimate the conditional distribution at a test point  $\mathbf{x}$  or any other quantity of interest. Suppose that we have built  $N$  trees  $T_1, \dots, T_N$ .

Let  $\mathcal{L}_k(\mathbf{x})$  be the set of the training data points which end up in the same leaf as  $\mathbf{x}$  in the tree  $T_k$ . The weighting function  $w_{\mathbf{x}}(\mathbf{x}_i)$  is defined as the average of the weighting functions per tree:

$$w_{\mathbf{x}}(\mathbf{x}_i) = \frac{1}{N} \sum_{k=1}^N \frac{\mathbb{1}(\mathbf{x}_i \in \mathcal{L}_k(\mathbf{x}))}{|\mathcal{L}_k(\mathbf{x})|}. \quad (2)$$

In the case of equally sized leaf nodes, the assigned weight to a training point  $x_i$  is proportional to the number of trees where the test point  $\mathbf{x}$  and  $\mathbf{x}_i$  end up in the same leaf node. We use the weighting function to define our estimate of the conditional distribution  $\mathbb{P}(\mathbf{Y} | \mathbf{X} = \mathbf{x})$ , given by

$$\hat{\mathbb{P}}(\mathbf{Y} | \mathbf{X} = \mathbf{x}) = \sum_i w_{\mathbf{x}}(\mathbf{x}_i) \cdot \delta(\mathbf{y}_i), \quad (3)$$

where  $\delta(\mathbf{y}_i)$  is the point mass at  $\mathbf{y}_i$ . Using the induced weighting function for locally weighted estimation is different than the approach of averaging the noisy estimates obtained per tree [25], used in standard Random Forests [5]. Even though the two approaches are equivalent for conditional mean estimation, the former approach is often much more efficient for more complicated targets [2].

The weighting function is illustrated in Figure 1. We obtained 5 years (2015 – 2019) of air pollution measurements from the US Environmental Protection Agency (EPA) website. 6 main air pollutants that form the air quality index (AQI) were measured at many different sites in USA for which we know the location, elevation, location setting (rural, urban, suburban) and how the land is used within a 1/4 mile radius. We want to know the distribution of the pollutant measurements at some new measurement site. The left plot illustrates how much weight in total do we assign to the measurements from a specific training site. We see that the important sites share many characteristics with the test site and DRF determines the relevance of each characteristic in a data-adaptive way.

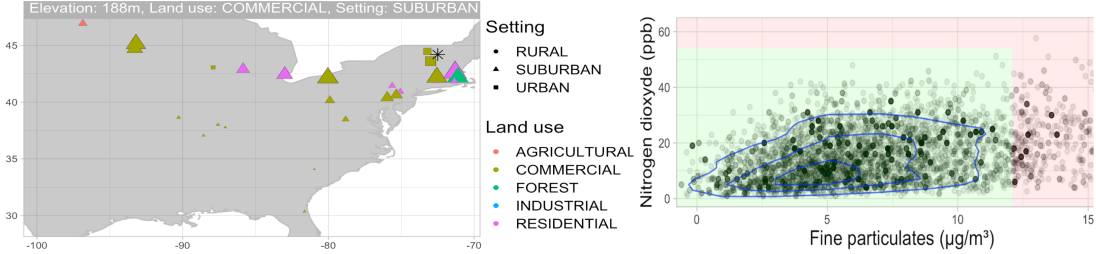


Figure 1: Left: the characteristics of the important training sites, for a fixed test site whose position is indicated by a black star and whose characteristics are indicated in the title. The total weight assigned corresponds to the symbol size. Right: estimated joint conditional distribution of two pollutants  $\text{NO}_2$  and  $\text{PM}_{2.5}$ . Green area corresponds to 'Good' air quality category ( $\text{AQI} \leq 50$ ).

**Two sample test.** In order to determine the best split, i.e. such that the distributions of the responses  $\mathbf{Y}$  in the resulting child nodes differ the most, one needs a good metric  $d$  (see Equation 1). Testing equality of distributions from the corresponding samples is an old problem in statistics, but obtaining an efficient test for multivariate distributions has proven to be quite challenging [9, 3]. One successful proposal, commonly used in practice, is the Maximum Mean Discrepancy (MMD) statistic  $d_{\text{MMD}}$  [10] for two samples  $\{\mathbf{u}_1, \dots, \mathbf{u}_m\}$  and  $\{\mathbf{v}_1, \dots, \mathbf{v}_n\}$  given by:

$$d_{\text{MMD}}(\{\mathbf{u}_i\}_{i=1}^m, \{\mathbf{v}_i\}_{i=1}^n) = \frac{1}{m^2} \sum_{i,j} k(\mathbf{u}_i, \mathbf{u}_j) + \frac{1}{n^2} \sum_{i,j} k(\mathbf{v}_i, \mathbf{v}_j) - \frac{2}{mn} \sum_i \sum_j k(\mathbf{u}_i, \mathbf{v}_j), \quad (4)$$

where  $k$  is some kernel function. It compares the similarities within each sample with the similarities across samples. It is a very flexible test and is shown to be able to detect any change in distribution.

However, its  $\mathcal{O}((m+n)^2)$  complexity might be too large for some applications. For that reason, several fast approximations of the MMD have been suggested [11, 27]. The complexity of the two-sample test used in DRF is crucial for the overall method to be computationally efficient, since the splitting step is used extensively in the forest construction. We propose splitting based on a fast random approximation of the MMD, called FastMMD [29]. It is based on Bochner's theorem, which gives us that any bounded shift-invariant kernel can be written as  $k(\mathbf{x}, \mathbf{y}) = \int_{\mathbb{R}^d} e^{i\omega^T(\mathbf{x}-\mathbf{y})} d\mu(\omega)$ ,

i.e. as a Fourier transform of some measure  $\mu$ . This enables us (see the supplement) to write the MMD two-sample test statistic as

$$d_{\text{MMD}}(\{\mathbf{u}_i\}_{i=1}^m, \{\mathbf{v}_i\}_{i=1}^n) = \int_{\mathbb{R}^d} \left| \frac{1}{m} \sum_{i=1}^m \varphi_{\omega}(\mathbf{u}_i) - \frac{1}{n} \sum_{i=1}^n \varphi_{\omega}(\mathbf{v}_i) \right|^2 d\mu(\omega), \quad (5)$$

where  $\varphi_{\omega}(\mathbf{y}) = e^{i\omega^T \mathbf{y}} \in \mathbb{C}$  are the Fourier features. The above integral is approximated by Monte Carlo, where the frequency vector  $\omega$  is sampled  $B$  times from  $\mu$ , thus reducing the computational complexity to  $\mathcal{O}(B(m+n))$ . This finally leads to our splitting criterion:

$$\frac{1}{B} \sum_{k=1}^B \frac{n_L n_R}{n_P^2} \left| \frac{1}{n_L} \sum_{\mathbf{x}_i \in C_L} \varphi_{\omega_k}(\mathbf{y}_i) - \frac{1}{n_R} \sum_{\mathbf{x}_i \in C_R} \varphi_{\omega_k}(\mathbf{y}_i) \right|^2, \quad (6)$$

where  $n_P = |\{i \mid \mathbf{x}_i \in P\}|$  and  $n_L, n_R$  are defined analogously. The additional scaling factor  $\frac{n_L n_R}{n_P^2}$  occurs naturally and compensates the increased variance of the MMD for unbalanced splits. For a Gaussian kernel  $k$  with bandwidth  $\sigma$ , we have to sample  $\omega_1, \dots, \omega_B \sim N_d(\mathbf{0}, \sigma^{-2} I_d)$ . We choose  $\sigma = 1$  as the default value and we standardize our responses before building the trees to make the method scale invariant. Taking larger  $B$  brings the splitting criterion (6) closer to the MMD criterion, but in practice even smaller  $B$  performs well, which also has a big computational advantage.

There is some similarity of our splitting criterion with the standard variance reduction CART criterion when  $d = 1$ , which can be rewritten as  $\frac{n_L n_R}{n_P^2} \left| \frac{1}{n_L} \sum_{\mathbf{x}_i \in C_L} y_i - \frac{1}{n_R} \sum_{\mathbf{x}_i \in C_R} y_i \right|^2$  (derivation in the supplement). We see that CART criterion compares the means of the response in the child nodes, which shows that aggregating the marginal CART criteria [16] for multivariate applications can only detect changes in the marginal means. However, it is possible that the correlations or the variances of the responses change, while the marginal means stay (almost) constant (see Figure 5). Furthermore, aggregation over  $d$  responses might reduce the signal size if only a few components change. Our splitting criterion based on the MMD is able to avoid such difficulties.

Interestingly, the following theorem shows that the MMD splitting criterion can be viewed as the CART criterion in the RKHS  $\mathcal{H}$  corresponding to  $k$  [7]. Moreover, we see that asymptotically DRF with the MMD splitting criterion can be viewed as greedy minimization of the squared distance between the corresponding embeddings of our estimate  $\hat{\mathbb{P}}(\mathbf{Y} \mid \mathbf{X})$  and the truth  $\mathbb{P}(\mathbf{Y} \mid \mathbf{X})$  in  $\mathcal{H}$ .

**Theorem 1.** *Let  $\mathcal{H}$  be the RKHS corresponding to a bounded kernel  $k$  and for any distribution  $\mathcal{D}$ , let  $\mu(\mathcal{D})$  be its embedding into  $\mathcal{H}$ . Furthermore, for a split of parent node  $P$  into  $C_L$  and  $C_R$ , let  $\hat{\mathbb{P}}_{\text{split}}(\mathbf{x}) = \sum_{j \in \{L, R\}} \mathbb{1}(\mathbf{x} \in C_j) \frac{1}{n_j} \sum_{i \in C_j} \delta_{\mathbf{y}_i}$  be the empirical distribution of  $\mathbf{Y}$  at  $\mathbf{x}$ . Then:*

$$\arg \max_{\text{split}} d_{\text{MMD}}(\{\mathbf{y}_i \mid \mathbf{x}_i \in C_L\}, \{\mathbf{y}_i \mid \mathbf{x}_i \in C_R\}) = \arg \min_{\text{split}} \frac{1}{n_P} \sum_{\mathbf{x}_i \in P} \left\| \mu(\delta_{\mathbf{y}_i}) - \mu(\hat{\mathbb{P}}_{\text{split}}(\mathbf{x}_i)) \right\|_{\mathcal{H}}^2.$$

$$\frac{1}{n_P} \sum_{\mathbf{x}_i \in P} \left\| \mu(\delta_{\mathbf{y}_i}) - \mu(\hat{\mathbb{P}}(\mathbf{x}_i)) \right\|_{\mathcal{H}}^2 = V(P) + \mathbb{E} \left[ \left\| \mu(\hat{\mathbb{P}}(\mathbf{X})) - \mu(\mathbb{P}(\mathbf{Y} \mid \mathbf{X})) \right\|_{\mathcal{H}}^2 \mid \mathbf{X} \in P \right] + \mathcal{O}_p(n^{-1/2}),$$

where  $V(P) = \mathbb{E} \left[ \left\| \mu(\delta_{\mathbf{Y}}) - \mu(\mathbb{P}(\mathbf{Y} \mid \mathbf{X})) \right\|_{\mathcal{H}}^2 \mid \mathbf{X} \in P \right]$  is a deterministic term not depending on  $\hat{\mathbb{P}}$ .

**Two-step framework.** In addition to estimating the joint conditional distribution, the weighting function  $w_{\mathbf{x}}(\mathbf{x}_i)$  can directly be used for other quantities of interest in a second step. For example, the estimated conditional joint cumulative distribution function is given by  $\hat{\mathbb{P}}(Y_1 \leq c_1, \dots, Y_d \leq c_d \mid \mathbf{X} = \mathbf{x}) = \sum_i w_{\mathbf{x}}(\mathbf{x}_i) \mathbb{1}((\mathbf{y}_i)_1 \leq c_1, \dots, (\mathbf{y}_i)_d \leq c_d)$ . Many other quantities such as, for example, conditional quantiles, conditional correlations or various conditional probability statements can similarly be directly estimated from the weights.

By using the weights as an input for some other method, we might even accomplish some more complicated objectives, such as conditional independence testing, causal effect estimation, semiparametric learning, time series prediction or tail-index estimation in extremes modeling. As an example, suppose that our data  $\mathbf{Y}$  come from a parametric model, where the parameter  $\theta$  is not constant, but depends on  $\mathbf{X}$  instead, i.e.  $\mathbf{Y} \mid \mathbf{X} = \mathbf{x} \sim f(\theta(\mathbf{x}), \cdot)$ . One can then estimate the parameter  $\theta(\mathbf{x})$  by

using the weighted MLE:  $\hat{\theta}(\mathbf{x}) = \arg \max_{\theta} \sum_i w_{\mathbf{x}}(\mathbf{x}_i) \log f(\theta, \mathbf{y}_i)$ , where the weighting function  $w_{\mathbf{x}}$  is obtained from DRF.

An illustration of using DRF as a two step method is given in Figure 2: in the first step we obtain the weighting function  $w_{\mathbf{x}}(\cdot)$ , which is then used as an input for the second step. Even if the method used in the second step does not directly support weighting of the training data points, one can easily resample the data set according to  $w_{\mathbf{x}}(\cdot)$ .

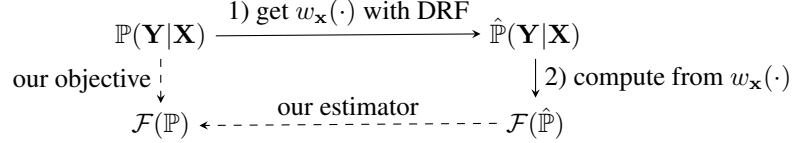


Figure 2: Illustration of the two-step procedure using DRF. One first gets the weights which describe the conditional distribution, which are then used for computing the target quantity.

### 3 Illustrations and numerical experiments

We demonstrate in this section how DRF can provide insight into distributional heterogeneity. We investigate the performance of the resulting out-of-the-box estimators for multivariate distributions and illustrate the usefulness of DRF for many different applications. Detailed descriptions of all data sets and the corresponding analyses can be found in the supplement.

**Statistical functionals.** Because DRF represents the estimated conditional distribution  $\hat{\mathbb{P}}(\mathbf{Y} | \mathbf{X} = \mathbf{x}) = \sum_i w_{\mathbf{x}}(\mathbf{x}_i) \cdot \delta_{\mathbf{y}_i}$  in a convenient form by using weights  $w_{\mathbf{x}}(\mathbf{x}_i)$ , a plug-in estimator  $\mathcal{F}(\hat{\mathbb{P}}(\mathbf{Y} | \mathbf{X} = \mathbf{x}))$  of many statistical functionals  $\mathcal{F}(\mathbb{P}(\mathbf{Y} | \mathbf{X} = \mathbf{x}))$  can be easily constructed. In Figure 3 we see the estimated probability that the air quality index (AQI) is at most 50. This corresponds to the "Good" category and means that the amount of each air pollutant is below a certain threshold determined by the EPA.

In addition to the classical functionals in the form of the expectation  $\mathbb{E}(f(\mathbf{Y}) | \mathbf{X} = \mathbf{x})$  or a quantile  $Q_{\alpha}(f(\mathbf{Y}) | \mathbf{X} = \mathbf{x})$  for a function  $f : \mathbb{R}^d \rightarrow \mathbb{R}$  (which can be recast as one-dimensional problems), additional interesting statistical functionals with intrinsically multivariate nature are accessible by DRF, e.g. the conditional correlations  $\text{Corr}(Y_i, Y_j | \mathbf{X} = \mathbf{x})$ . The estimated correlation of the sulfur dioxide ( $\text{SO}_2$ ) and fine particulate matter ( $\text{PM}_{2.5}$ ) is shown in Figure 3. We can see that the correlation in many big cities is slightly larger than in its surroundings, which is reasonable because the industrial production directly affects the levels of both pollutants.

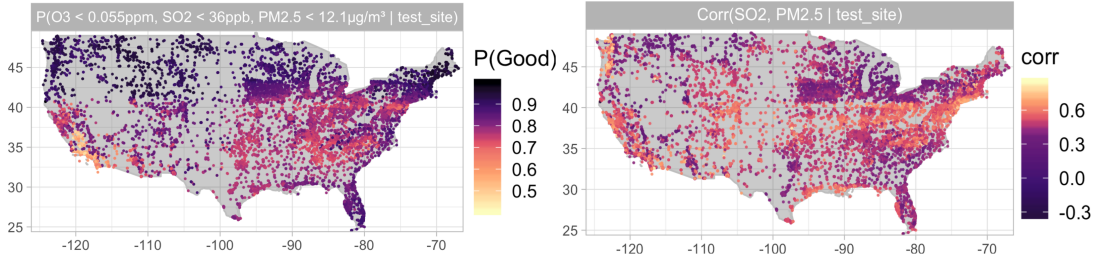


Figure 3: Estimates of the conditional CDF (left), corresponding to  $\mathbb{P}(\text{AQI} \leq 50)$ , and the conditional correlation (right) derived from the DRF estimate of the multivariate conditional distribution.

In practice, estimating statistical functionals from the weights provided by DRF comes at a minimal loss compared to the benchmark methods specifically designed for this task. In Figure 4 we can see that the DRF estimates of the  $\mathbb{P}(\text{AQI} \leq 50)$  (illustrated also in Figure 3) are quite similar to the estimates of the classification forest [5] predicting the outcome  $\mathbb{1}(\text{AQI} \leq 50)$ . Furthermore, the cross-entropy loss evaluated on held-out measurements equals 0.4671 and 0.4663 respectively, showing almost no loss of precision.

On the other hand, using DRF approach has many advantages. Many quantities, e.g. conditional correlations, are not that simple to estimate directly. Secondly, using DRF has great computational advantage: one only needs to learn the weighting function  $w_{\mathbf{x}}$  once in order to estimate many different targets, whereas, as an example, estimating the cumulative distribution function with classification forests requires fitting one forest for each function value. Finally, since all statistical functionals are plug-in estimates from the same weighting function, the obtained estimates are well-behaved and satisfy required mathematical properties. As an illustration, Figure 4 shows that the estimated cumulative distribution function (CDF) using the classification forest need not be monotone due to random errors in each predicted value, which can not happen with the DRF estimates.

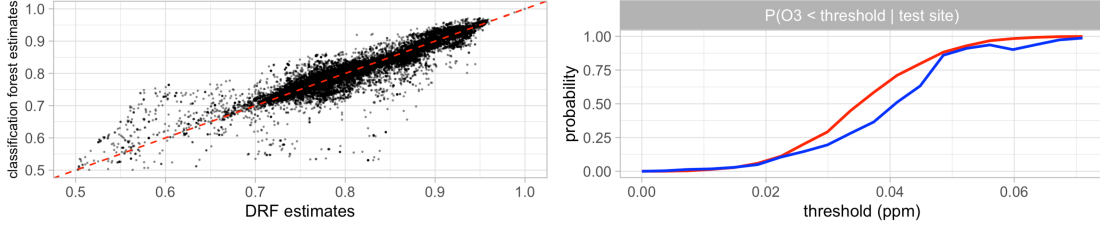


Figure 4: Left: Comparison of the CDF estimates obtained by DRF (displayed also in the left plot of Figure 3) and by the classification forest. Right: Example how the CDF estimated by using the classification forest (blue) need not be monotone, whereas the DRF estimates (red) are well-behaved.

**Conditional copulas.** The well-known Sklar’s theorem [24] implies that at a point  $\mathbf{x} \in \mathbb{R}^p$ , the conditional CDF  $\mathbb{P}(\mathbf{Y} \leq \mathbf{y} | \mathbf{X} = \mathbf{x}) = \mathbb{P}(Y_1 \leq y_1, \dots, Y_d \leq y_d | \mathbf{X} = \mathbf{x})$  can be represented by a CDF  $C_{\mathbf{x}}$  on  $[0, 1]^d$ , the conditional copula at  $\mathbf{x}$ , and  $d$  conditional marginal CDFs  $F_i(y | \mathbf{X} = \mathbf{x}) = \mathbb{P}(Y_i \leq y | \mathbf{X} = \mathbf{x})$  for  $1 \leq i \leq d$ , as follows:

$$\mathbb{P}(Y_1 \leq y_1, \dots, Y_d \leq y_d | \mathbf{X} = \mathbf{x}) = C_{\mathbf{x}}(F_1(y_1 | \mathbf{x}), \dots, F_d(y_d | \mathbf{x})). \quad (7)$$

From this decomposition one can see that distributional heterogeneity can not only occur in marginal distribution of the responses (a case extensively studied in the literature), but also in their interdependence structure through the conditional copula  $C_{\mathbf{x}}$ . Since DRF relies on a joint distribution metric for its splitting criterion, it is capable of detecting any change in distribution, whereas aggregating marginal criteria for  $Y_1, \dots, Y_d$  only captures the changes in marginal distributions.

To illustrate this, consider an example where the bivariate response is generated from the Gaussian copula  $\mathbf{Y} = (Y_1, Y_2) | \mathbf{X} = \mathbf{x} \sim C_{\rho(\mathbf{x})}^{\text{Gauss}}$  conditionally on the covariates  $X_1, \dots, X_{100} \stackrel{i.i.d.}{\sim} U(-1, 1)$ .  $Y_1$  and  $Y_2$  both have  $N(0, 1)$  distribution marginally, but their correlation is given by  $\rho(\mathbf{x}) = x_1$ . The results are displayed in Figure 5. We see that DRF is able to recover the full conditional distribution well for any point of interest  $\mathbf{x}$ . This estimated distribution can further be used to estimate the conditional correlation  $\text{Corr}(Y_1, Y_2 | \mathbf{X} = \mathbf{x})$  and to test the conditional independence  $Y_1 \perp Y_2 | \mathbf{X} = \mathbf{x}$  with HSIC [12]. We see that DRF with the MMD based splitting rule (6) performs better than the DRF with the sum of CART criteria; it estimates the correlation more accurately and the HSIC test statistic is much larger as  $Y_1, Y_2$  get more dependent.

**Benchmark data sets.** We now compare the performance of DRF with several competing methods for estimation of multivariate distributions. We combine the benchmark data sets from the multi-target regression literature [1] with additional ones based on the data sets described in this paper. Since our target is not just conditional mean, but the entire distribution, a special distributional loss is used: for 100 random univariate linear projections of the response  $\mathbf{Y}$ , we compute 0.9 quantile (pinball) loss for the resulting quantile estimates. Table 1 records the average rank across the projections. We see that DRF performs well for a wide range of sample size and problem dimensionality. All competing methods, data sets and the loss function are described in detail in the supplement.

**Heterogeneous regression.** Suppose we want to infer the relationship between some target quantity  $Y$  and certain explanatory variables  $\mathbf{W}$  from heterogeneous data, where the heterogeneity is caused by some known variables  $\mathbf{Z}$ . This problem is hard; not only can the marginal distributions of  $Y$  and  $\mathbf{W}$  be affected by  $\mathbf{Z}$ , thus inducing spurious associations due to confounding, but the mechanism how

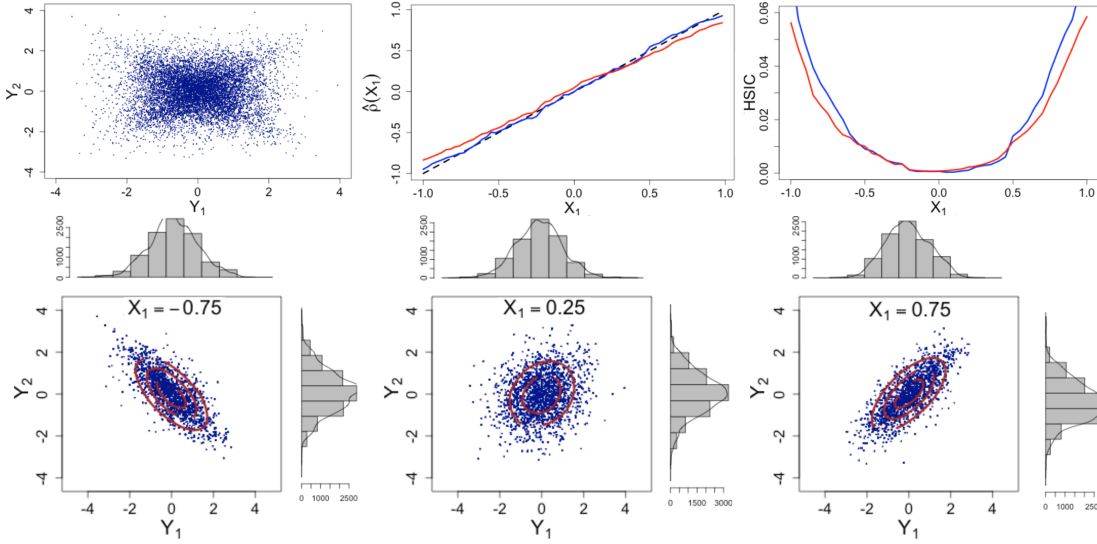


Figure 5: Bottom row: 10'000 samples drawn from the estimated conditional distributions at  $\mathbf{x}$  when  $x_1$  equals  $-0.9, 0$  and  $0.9$  respectively and other covariates equal zero. Top row: pooled training responses (left), estimated conditional correlation  $\hat{\rho}$  (middle) and conditional dependence of  $Y_1$  and  $Y_2$  quantified by HSIC (right), estimated by  $\text{DRF}_{\text{MMD}}$  (blue) and  $\text{DRF}_{\text{CART}}$  (red) respectively.

	jura	slump	wq	enb	atp1d	atp7d	scpf	sf1	sf2	copula	wage	births1	births2	air
$n$	359	103	1K	768	337	296	143	323	1K	5K	10K	10K	10K	10K
$p$	15	7	16	8	370	370	8	21	22	10	73	23	24	15
$d$	3	3	14	2	6	6	3	3	6	2	2	2	4	6
$\text{DRF}_{\text{MMD}}$	1.9	2.5	1.9	1.8	2.6	2.8	2.5	<b>2</b>	<b>2.6</b>	<b>1.3</b>	<b>1.5</b>	<b>1</b>	1.65	2
$\text{DRF}_{\text{CART}}$	<b>1.5</b>	<b>1.7</b>	<b>1.1</b>	<b>1.1</b>	<b>1.6</b>	1.9	<b>2.2</b>	2.9	3.3	2.2	<b>1.5</b>	2	<b>1.3</b>	<b>1</b>
Homogeneous	4.9	4.3	4.2	4.8	4.5	4.4	4	3.7	3	4.2	4	4.2	4.3	4.7
k-NN	2.6	2	3	3	1.8	<b>1.2</b>	2.6	2.7	3	3.6	3	3	3	3
Gauss kernel	4.1	4.4	4.7	4.1	4.3	4.5	3.5	3.6	3	3.6	5	4.8	4.6	4.3

Table 1: Average rank with respect to the 0.9 quantile (pinball) loss for the induced 0.9-quantile estimates across 100 random linear projections. The best method is highlighted in bold.

$\mathbf{W}$  affects  $Y$  can itself depend on  $\mathbf{Z}$ . One way to approach this problem with DRF is to first estimate the joint distribution of  $(\mathbf{W}, Y)$  conditionally on  $\mathbf{Z}$  and then use the weighting function  $w_{\mathbf{z}}$  with an appropriate method for regressing  $Y$  on  $\mathbf{W}$  in the second step. In this way one can efficiently exploit and incorporate any prior knowledge of the relationship between  $\mathbf{W}$  and  $Y$ , such as e.g. monotonicity, smoothness or that it satisfies certain parametric regression model.

We illustrate this on the natality data obtained from the CDC website, where we have information about all recorded births in the USA in 2018. We investigate the relationship between the pregnancy length and the birthweight, an important indicator of baby's health. However, this relationship is not fixed and depends on many different factors, such as parents' race, baby's gender, birth multiplicity etc. In Figure 6 one can see the estimated joint distribution of birthweight and pregnancy length conditionally on many potential confounders indicated in the plot. The black curves denote the subsequent regression fit, based on the smoothing splines, together with the estimates of the conditional 0.1 and 0.9 quantiles, with which one can determine whether a baby is large or small for its gestational age. Notice how DRF assigns less importance to the mother's race when the point of interest is a twin (middle plot); in this case more weight is given to twin births, regardless of the race.

Suppose now we would like to know what is the direct effect of a twin birth  $T$  on the birthweight  $B$ , ignoring the indirect effect due to shorter pregnancy length  $L$ , when other confounding variables  $\mathbf{Z}$ , e.g. the parents' race, can affect  $B, T$  and  $L$ . This causal graph is displayed in the supplement. In



order to adjust for the confounding, we are interested in the following causal quantity:

$$\begin{aligned}\mathbb{P}(B \mid do(T = t, L = l)) &= \int \mathbb{P}(B \mid do(T = t, L = l), \mathbf{Z} = \mathbf{z}) \mathbb{P}(\mathbf{Z} = \mathbf{z} \mid do(T = t, L = l)) d\mathbf{z} \\ &= \int \mathbb{P}(B \mid T = t, L = l, \mathbf{Z} = \mathbf{z}) \mathbb{P}(\mathbf{Z} = \mathbf{z}) d\mathbf{z}.\end{aligned}\quad (8)$$

The first term can be computed from the DRF with the subsequent regression fits, which also has the advantage that we can better extrapolate to regions with small probability, such as long twin pregnancies. In the right plot of Figure 6 we show the mean and quantiles of the estimated interventional distribution and we see that, as one might expect, a twin birth causes smaller birthweight on average, with the difference increasing with the length of the pregnancy.

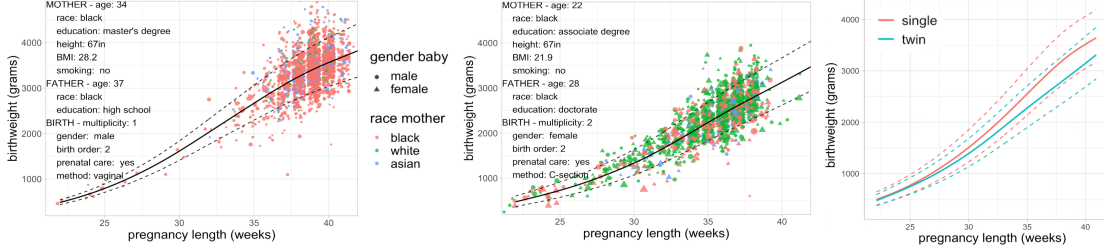


Figure 6: Left and middle: estimated relationship of pregnancy length and birthweight, conditionally on the criteria indicated in the upper left corner. Right: estimated interventional effect of twin birth on the birthweight for a fixed pregnancy length. In all plots the solid curves denote the estimated conditional mean and the dashed denote the estimated 0.1 and 0.9 quantiles.

**Fairness.** Being able to compute different causal quantities with DRF could prove useful in a range of applications, including fairness [18]. We investigate the data on approximately 1 million full-time employed people from the 2018 American Community Survey carried out by the US Census Bureau. We want to answer whether the observed gender pay gap in the data can at least in part be explained by other factors, such as the job type, age, children, geography, race, educational attainment and many others. In order to determine the direct effect of the gender  $G$  on wage  $W$  that is not mediated by other factors  $\mathbf{Z}$ , we compute the distribution of the nested counterfactual

$$\begin{aligned}\mathbb{P}(W(\text{male}, \mathbf{Z}(\text{female}))) &= \int \mathbb{P}(W \mid do(\mathbf{Z} = \mathbf{z}, G = \text{male})) \mathbb{P}(\mathbf{Z} = \mathbf{z} \mid do(G = \text{female})) d\mathbf{z} \\ &= \int \mathbb{P}(W \mid \mathbf{Z} = \mathbf{z}, G = \text{male}) \mathbb{P}(\mathbf{Z} = \mathbf{z} \mid G = \text{female}) d\mathbf{z},\end{aligned}\quad (9)$$

which quantifies the gender discrimination when all variables  $\mathbf{Z}$  are taken to be resolving [15]. It can be interpreted as the distribution of the women's wages had they been treated as men for determining the salary, without changing their other characteristics, such as the choice of occupation. By computing first the joint distribution of  $(W, G)$  conditionally on  $\mathbf{Z}$  with DRF, this counterfactual distribution can be easily computed from Equation (9). In the middle panel of Figure 7 we see a noticeable difference in the means, called also natural direct effect in causal literature [20], between the observed distribution of women's salaries and the hypothetical distribution of their salaries had they been men. By matching the corresponding quantiles of those two distributions [21] in the right panel, we can see that the adjusted gender pay gap even increases for larger salaries. Median hourly wage for women is 11% lower than the median wage for the adjusted population of men with exactly the same characteristics  $\mathbf{Z}$  as women, indicating that only a small proportion of the actually observed hourly wage difference of 17% can be explained by other demographic factors.

## 4 Conclusion

We have shown that DRF is a flexible, general and powerful tool, which can not only estimate conditional and possibly multivariate distributions, but can also be used as out-of-the-box algorithm for many learning problems in a wide range of applications, including also causality and fairness.





Figure 7: Estimated joint distribution of wage and gender for a given value of factors (left). Estimated counterfactual distribution of women’s salaries had they been men (middle) and the quantile comparison with the observed salary distribution (right).

## References

- [1] Mulan: A java library for multi-label learning. <http://mulan.sourceforge.net/datasets-mtr.html>. Accessed: 2020-05-18.
- [2] Susan Athey, Julie Tibshirani, Stefan Wager, et al. Generalized random forests. *The Annals of Statistics*, 47(2):1148–1178, 2019.
- [3] Ludwig Baringhaus and Carsten Franz. On a new multivariate two-sample test. *Journal of multivariate analysis*, 88(1):190–206, 2004.
- [4] Peter J Bickel, Chris AJ Klaassen, Ya’acov Ritov, and Jon A Wellner. *Efficient and adaptive estimation for semiparametric models*, volume 4. Johns Hopkins University Press Baltimore, 1993.
- [5] Leo Breiman. Random forests. *Machine learning*, 45(1):5–32, 2001.
- [6] William S Cleveland. Robust locally weighted regression and smoothing scatterplots. *Journal of the American statistical association*, 74(368):829–836, 1979.
- [7] Guangzhe Fan, Zhou Wang, and Jiheng Wang. Cw-ssim kernel based random forest for image classification. In *Visual Communications and Image Processing 2010*, volume 7744, page 774425. International Society for Optics and Photonics, 2010.
- [8] Jianqing Fan, Mark Farnen, and Irene Gijbels. Local maximum likelihood estimation and inference. *Journal of the Royal Statistical Society: Series B (Statistical Methodology)*, 60(3):591–608, 1998.
- [9] Jerome H Friedman and Lawrence C Rafsky. Multivariate generalizations of the wald-wolfowitz and smirnov two-sample tests. *The Annals of Statistics*, pages 697–717, 1979.
- [10] Arthur Gretton, Karsten Borgwardt, Malte Rasch, Bernhard Schölkopf, and Alex J Smola. A kernel method for the two-sample-problem. In *Advances in neural information processing systems*, pages 513–520, 2007.
- [11] Arthur Gretton, Karsten M Borgwardt, Malte J Rasch, Bernhard Schölkopf, and Alexander Smola. A kernel two-sample test. *Journal of Machine Learning Research*, 13(Mar):723–773, 2012.
- [12] Arthur Gretton, Kenji Fukumizu, Choon Hui Teo, Le Song, Bernhard Schölkopf, and Alexander J. Smola. A kernel statistical test of independence. In *Proceedings of the 20th International Conference on Neural Information Processing Systems, NIPS’07*, page 585–592, Red Hook, NY, USA, 2007. Curran Associates Inc.
- [13] Torsten Hothorn, Peter Bühlmann, Sandrine Dudoit, Annette Molinaro, and Mark J Van Der Laan. Survival ensembles. *Biostatistics*, 7(3):355–373, 2006.
- [14] Torsten Hothorn and Achim Zeileis. Transformation forests. *arXiv preprint arXiv:1701.02110*, 2017.
- [15] Niki Kilbertus, Mateo Rojas Carulla, Giambattista Parascandolo, Moritz Hardt, Dominik Janzing, and Bernhard Schölkopf. Avoiding discrimination through causal reasoning. In *Advances in Neural Information Processing Systems*, pages 656–666, 2017.
- [16] Dragi Kocev, Celine Vens, Jan Struyf, and Sašo Džeroski. Ensembles of multi-objective decision trees. In *European conference on machine learning*, pages 624–631. Springer, 2007.
- [17] Sören R Künzel, Jasjeet S Sekhon, Peter J Bickel, and Bin Yu. Metalearners for estimating heterogeneous treatment effects using machine learning. *Proceedings of the national academy of sciences*, 116(10):4156–4165, 2019.
- [18] Matt J Kusner, Joshua Loftus, Chris Russell, and Ricardo Silva. Counterfactual fairness. In *Advances in Neural Information Processing Systems*, pages 4066–4076, 2017.

- [19] Nicolai Meinshausen. Quantile regression forests. *Journal of Machine Learning Research*, 7(Jun):983–999, 2006.
- [20] Judea Pearl. *Causality*. Cambridge university press, 2009.
- [21] Drago Plečko and Nicolai Meinshausen. Fair data adaptation with quantile preservation. *arXiv preprint arXiv:1911.06685*, 2019.
- [22] Mark Segal and Yuanyuan Xiao. Multivariate random forests. *Wiley Interdisciplinary Reviews: Data Mining and Knowledge Discovery*, 1(1):80–87, 2011.
- [23] Bernard W Silverman. *Density estimation for statistics and data analysis*, volume 26. CRC press, 1986.
- [24] M. Sklar. *Fonctions de Répartition À N Dimensions Et Leurs Marges*. Université Paris 8, 1959.
- [25] Stefan Wager and Susan Athey. Estimation and inference of heterogeneous treatment effects using random forests. *Journal of the American Statistical Association*, 113(523):1228–1242, 2018.
- [26] Marvin N Wright and Andreas Ziegler. ranger: A fast implementation of random forests for high dimensional data in c++ and r. *arXiv preprint arXiv:1508.04409*, 2015.
- [27] Wojciech Zaremba, Arthur Gretton, and Matthew Blaschko. B-test: A non-parametric, low variance kernel two-sample test. In *Advances in neural information processing systems*, pages 755–763, 2013.
- [28] Kun Zhang, Jonas Peters, Dominik Janzing, and Bernhard Schölkopf. Kernel-based conditional independence test and application in causal discovery. *arXiv preprint arXiv:1202.3775*, 2012.
- [29] Ji Zhao and Deyu Meng. Fastmmd: Ensemble of circular discrepancy for efficient two-sample test. *Neural computation*, 27(6):1345–1372, 2015.

# Supplementary Material for Distributional Random Forests

**Domagoj Ćevd\***

ETH Zürich  
cevid@stat.math.ethz.ch

**Loris Michel\***

ETH Zürich  
michel@stat.math.ethz.ch

**Nicolai Meinshausen**

ETH Zürich  
meinshausen@stat.math.ethz.ch

**Peter Bühlmann**

ETH Zürich  
peter.buehlmann@stat.math.ethz.ch

## 1 Implementation details

Here we present in detail the implementation of the Distributional Random Forests (DRF). The code is available as the R-package `drf` and the Python package `drf`. The implementation is based on the implementations of the R-packages `grf` [?] and `ranger` [?]. The largest difference is in the splitting criterion itself. The pseudocode for the forest construction and computation of the weighting function  $w_{\mathbf{x}}(\cdot)$  is given in the Algorithm 1.

- Every tree is constructed based on a random subset of size  $s$  (taken to be 50% of the size of the training set by default) of the training data set [?]. This differs from the original Random Forest algorithm [?], where the bootstrap subsampling is done by drawing from the original sample with replacement.
- The principle of honesty [?, ?, ?] is used for building the trees (line 4), where for each tree one first performs the splitting based on one random set of data points  $\mathcal{S}_{\text{build}}$ , and then populates the leaves with a disjoint random set  $\mathcal{S}_{\text{populate}}$  of data points for determining the weighting function  $w_{\mathbf{x}}(\cdot)$ . This prevents overfitting, since we do not assign weight to the data points which we used to build the tree.
- We borrow the method for selecting the number of candidate splitting variables from the `grf` package [?]. This number is randomly generated as  $\min(\max(\text{Poisson}(\text{mtry}), 1), p)$ , where `mtry` is a tuning parameter. This differs from the original Random Forests algorithm, where the number of splitting candidates is fixed to be `mtry`.
- The number of trees built is  $N = 2000$  by default.
- The factor variables in both the responses and the predictors are encoded by using the one-hot encoding, where we add an additional indicator variable for each level  $l$  of some factor variable  $X_i$ . This implies that in the building step, if we split on this indicator variable, we divide the current set of data points in the sets where  $X_i = l$  and  $X_i \neq l$ . This works well if the number of levels is not too big, since otherwise one makes very uneven splits and the dimensionality of the problem increases significantly. Handling this issue is a well-known practical issue [?] and is a topic of our future work.
- We try to enforce splits where each children has at least a fixed percentage (chosen to be 10% as the default value) of the current number of data points. In this way we achieve balanced splits and reduce the computational time. However, we can not enforce this if we are trying to split on the variable  $X_i$  with only a few unique values, e.g. indicator variable for a level of some factor variable.

---

\*Alphabetical order, equal contribution of authors.

- All components of the response  $Y$  are scalend for the building step (but not when we populate the leaves). This ensures that each component of the response contributes equally to the kernel values, and consequently to the MMD two-sample test statistic.
- By default, in the step 20 of the Algorithm 1, we use the MMD-based splitting criterion given by

$$\frac{1}{B} \sum_{k=1}^B \frac{|\mathcal{S}_L| |\mathcal{S}_R|}{(|\mathcal{S}_L| + |\mathcal{S}_R|)^2} \left| \frac{1}{|\mathcal{S}_L|} \sum_{(\mathbf{x}_i, \mathbf{y}_i) \in \mathcal{S}_L} \varphi_{\omega_k}(\mathbf{y}_i) - \frac{1}{|\mathcal{S}_R|} \sum_{(\mathbf{x}_i, \mathbf{y}_i) \in \mathcal{S}_R} \varphi_{\omega_k}(\mathbf{y}_i) \right|^2$$

The Gaussian kernel  $k(\mathbf{x}, \mathbf{y}) = \frac{1}{(\sqrt{2\pi}\sigma)^d} e^{-\frac{\|\mathbf{x}-\mathbf{y}\|_2^2}{2\sigma^2}}$  with the bandwidth  $\sigma = 1$  is used as the default choice. However the algorithm works with any choice of the kernel, or in fact with any two-sample test.

---

**Algorithm 1** Distributional Random Forest

---

```

1: procedure BUILDFOREST(set of samples  $\mathcal{S} = \{(\mathbf{x}_i, \mathbf{y}_i)\}_{i=1}^n$ , number of trees  $N$ )
2:   for  $i = 1, \dots, N$  do
3:      $\mathcal{S}_{\text{subsample}} = \text{SUBSAMPLE}(\mathcal{S})$ 
4:      $\mathcal{S}_{\text{build}}, \mathcal{S}_{\text{populate}} \leftarrow \text{SPLITSAMPLES}(\mathcal{S}_{\text{subsample}})$   $\triangleright$  This is called honesty, see below
5:      $\mathcal{T}_i \leftarrow \text{CREATENETREE}(\mathcal{S}_{\text{build}})$   $\triangleright$  Samples  $\mathcal{S}_{\text{build}}$  are used for building the tree
6:      $\text{BUILDTREE}(\text{ROOTNODE}(\mathcal{T}_i))$   $\triangleright$  Start recursion from the root node
7:      $\text{POPULATELEAVES}(\mathcal{T}_i, \mathcal{S}_{\text{populate}})$   $\triangleright$  Only samples  $\mathcal{S}_{\text{populate}}$  are used for computing  $w_{\mathbf{x}}(\cdot)$ 
8:   end for
9:   return  $\mathcal{F} = \{\mathcal{T}_1, \dots, \mathcal{T}_N\}$ 
10: end procedure

11: procedure BUILDTREE(current node  $\mathcal{N}$ )  $\triangleright$  Recursively constructs the trees
12:   if STOPPINGCRITERION( $\mathcal{N}$ ) then  $\triangleright$  E.g. if only a few samples left
13:     return
14:   end if
15:    $\mathcal{S} \leftarrow \text{GETSAMPLES}(\mathcal{N})$ 
16:    $\mathcal{I} \leftarrow \text{GETSPLITVARIABLES}()$   $\triangleright$  Random set of candidate variables
17:    $\mathcal{C} \leftarrow \text{INITIALIZESPLITS}()$   $\triangleright$  Here we store info about candidate splits
18:   for  $\text{idx} \in \mathcal{I}$ , level  $l$  do  $\triangleright$   $l$  iterates over all values of variable  $X_{\text{idx}}$ 
19:      $\mathcal{S}_L, \mathcal{S}_R \leftarrow \text{CHILDSAMPLES}(\mathcal{S}, \text{idx}, l)$   $\triangleright$  Splits samples based on whether  $(\mathbf{x}_i)_{\text{idx}} \leq l$ 
20:     test statistic value  $v = \text{SPLITTINGCRITERION}(\mathcal{S}_L, \mathcal{S}_R)$   $\triangleright$  Two-sample test of choice
21:      $\text{ADDNEWSPLITCANDIDATE}(\mathcal{C}, v, \mathcal{S}_L, \mathcal{S}_R, \text{idx}, l)$ 
22:   end for
23:    $\mathcal{S}_L, \mathcal{S}_R, \text{idx}, l \leftarrow \text{FINDBESTSPLIT}(\mathcal{C})$ 
24:    $\mathcal{N}_L \leftarrow \text{CREATENODE}(\mathcal{S}_L)$   $\triangleright$  Create new node with set of samples  $\mathcal{S}_L$ 
25:    $\mathcal{N}_R \leftarrow \text{CREATENODE}(\mathcal{S}_R)$   $\triangleright$  Create new node with set of samples  $\mathcal{S}_R$ 
26:    $\text{BUILDTREE}(\mathcal{N}_L), \text{BUILDTREE}(\mathcal{N}_R)$   $\triangleright$  Proceed building recursively
27:    $\text{CHILDREN}(\mathcal{N}) \leftarrow \mathcal{N}_L, \mathcal{N}_R$ 
28:    $\text{SPLIT}(\mathcal{N}) \leftarrow \text{idx}, l$   $\triangleright$  Store the split
29:   return
30: end procedure

31: procedure GETWEIGHTS(forest  $\mathcal{F}$ , test point  $\mathbf{x}$ )  $\triangleright$  Computes the weighting function  $w_{\mathbf{x}}(\cdot)$ 
32:   vector of weights  $w = \text{ZEROS}(n)$   $\triangleright$   $n$  is the training set size
33:   for  $i = 1, \dots, |\mathcal{F}|$  do
34:      $\mathcal{L} = \text{GETLEAFSAMPLES}(\mathcal{T}_i, \mathbf{x})$   $\triangleright$  indices of all training samples in the same leaf as  $\mathbf{x}$ 
35:     for  $\text{idx} \in \mathcal{L}$  do
36:        $w[\text{idx}] = w[\text{idx}] + 1/(|\mathcal{L}| \cdot |\mathcal{F}|)$ 
37:     end for
38:   end for
39:   return  $w$ 
40: end procedure

```

---

## 2 Formulae derivations

### 2.1 MMD two-sample test statistic for shift-invariant kernel

The biased MMD two-sample statistic is given as

$$\begin{aligned} d_{\text{MMD}}(\{\mathbf{u}_i\}_{i=1}^m, \{\mathbf{v}_i\}_{i=1}^n) &= \frac{1}{m^2} \sum_{i,j} k(\mathbf{u}_i, \mathbf{u}_j) + \frac{1}{n^2} \sum_{i,j} k(\mathbf{v}_i, \mathbf{v}_j) - \frac{2}{mn} \sum_i \sum_j k(\mathbf{u}_i, \mathbf{v}_j) \\ &= \frac{1}{m^2} \sum_{i,j} k(\mathbf{u}_i, \mathbf{u}_j) + \frac{1}{n^2} \sum_{i,j} k(\mathbf{v}_i, \mathbf{v}_j) - \frac{1}{mn} \sum_i \sum_j k(\mathbf{u}_i, \mathbf{v}_j) - \frac{1}{mn} \sum_i \sum_j k(\mathbf{v}_j, \mathbf{u}_i) \end{aligned}$$

Assume that the kernel  $k$  is bounded and shift-invariant, then by Bochner's theorem there exist a measure  $\mu$  such that  $k$  can be written as  $k(\mathbf{x}, \mathbf{y}) = \int_{\mathbb{R}^d} e^{i\omega^T(\mathbf{x}-\mathbf{y})} d\mu(\omega)$ .

Let us write  $\varphi_{\omega}^U = \frac{1}{m} \sum_i e^{i\omega^T \mathbf{u}_i}$  and  $\varphi_{\omega}^V = \frac{1}{n} \sum_i e^{i\omega^T \mathbf{v}_i}$ . We can now write  $d_{\text{MMD}}$  as

$$\begin{aligned} d_{\text{MMD}} &= \int_{\mathbb{R}^d} \left( \frac{1}{m^2} \sum_{i,j} e^{i\omega^T(\mathbf{u}_i - \mathbf{u}_j)} + \frac{1}{n^2} \sum_{i,j} e^{i\omega^T(\mathbf{v}_i - \mathbf{v}_j)} - \frac{1}{mn} \sum_i \sum_j e^{i\omega^T(\mathbf{u}_i - \mathbf{v}_j)} - \frac{1}{mn} \sum_i \sum_j e^{i\omega^T(\mathbf{v}_j - \mathbf{u}_i)} \right) d\mu(\omega) \\ &= \int_{\mathbb{R}^d} \left( \varphi_{\omega}^U \overline{\varphi_{\omega}^U} + \varphi_{\omega}^V \overline{\varphi_{\omega}^V} - \varphi_{\omega}^U \overline{\varphi_{\omega}^V} - \varphi_{\omega}^V \overline{\varphi_{\omega}^U} \right) d\mu(\omega) = \int_{\mathbb{R}^d} |\varphi_{\omega}^U - \varphi_{\omega}^V|^2 d\mu(\omega) \\ &= \int_{\mathbb{R}^d} \left| \frac{1}{m} \sum_{i=1}^m \varphi_{\omega}(\mathbf{u}_i) - \frac{1}{n} \sum_{i=1}^n \varphi_{\omega}(\mathbf{v}_i) \right|^2 d\mu(\omega), \end{aligned}$$

where  $\varphi_{\omega}(\mathbf{y}) = e^{i\omega^T \mathbf{y}} \in \mathbb{C}$  are the corresponding Fourier features, which is what we wanted to show.

### 2.2 CART criterion rewritten

Standard CART criterion used in Random Forests [?] is the following: we repeatedly choose to split the parent node  $P$  of size  $n$  in two children  $C_L$  and  $C_R$ , of sizes  $n_L$  and  $n_R$  respectively, such that the expression

$$\frac{1}{n} \left( \sum_{i \in C_L} (Y_i - \bar{Y}_L)^2 + \sum_{i \in C_R} (Y_i - \bar{Y}_R)^2 \right) \quad (1)$$

is minimized, where  $\bar{Y}_L = \frac{1}{n_L} \sum_{i \in C_L} Y_i$  and  $\bar{Y}_R$  is defined similarly.

We now have  $\bar{Y} = \frac{1}{n} \sum_{i \in P} Y_i = \frac{n_L}{n} \bar{Y}_L + \frac{n_R}{n} \bar{Y}_R$ , which gives  $\bar{Y} - \bar{Y}_L = \frac{n_R}{n} (\bar{Y}_R - \bar{Y}_L)$ , so we can write

$$\begin{aligned} \sum_{i \in C_L} (Y_i - \bar{Y}_L)^2 &= \sum_{i \in C_L} (Y_i - \bar{Y} + \bar{Y} - \bar{Y}_L)^2 = \sum_{i \in C_L} (Y_i - \bar{Y} + \frac{n_R}{n} (\bar{Y}_R - \bar{Y}_L))^2 \\ &= \sum_{i \in C_L} (Y_i - \bar{Y})^2 + 2 \frac{n_R}{n} (\bar{Y}_R - \bar{Y}_L) \sum_{i \in C_L} (Y_i - \bar{Y}) + \frac{n_L n_R^2}{n^2} (\bar{Y}_R - \bar{Y}_L)^2 \\ &= \sum_{i \in C_L} (Y_i - \bar{Y})^2 + 2 \frac{n_R}{n} (\bar{Y}_R - \bar{Y}_L) \cdot n_L (\bar{Y}_L - \bar{Y}) + \frac{n_L n_R^2}{n^2} (\bar{Y}_R - \bar{Y}_L)^2 \\ &= \sum_{i \in C_L} (Y_i - \bar{Y})^2 + 2 \frac{n_R n_L}{n} (\bar{Y}_R - \bar{Y}_L) \cdot \frac{n_R}{n} (\bar{Y}_L - \bar{Y}_R) + \frac{n_L n_R^2}{n^2} (\bar{Y}_R - \bar{Y}_L)^2 \\ &= \sum_{i \in C_L} (Y_i - \bar{Y})^2 - \frac{n_L n_R^2}{n^2} (\bar{Y}_R - \bar{Y}_L)^2 \end{aligned}$$

Similarly we obtain

$$\sum_{i \in C_L} (Y_i - \bar{Y}_L)^2 = \sum_{i \in C_L} (Y_i - \bar{Y} + \bar{Y} - \bar{Y}_L)^2 = \sum_{i \in C_R} (Y_i - \bar{Y})^2 - \frac{n_L^2 n_R}{n^2} (\bar{Y}_R - \bar{Y}_L)^2,$$

which gives us that the CART criterion (1) can be written as

$$\begin{aligned} \frac{1}{n} \left( \sum_{i \in C_L} (Y_i - \bar{Y})^2 - \frac{n_L n_R^2}{n^2} (\bar{Y}_R - \bar{Y}_L)^2 + \sum_{i \in C_R} (Y_i - \bar{Y})^2 - \frac{n_L^2 n_R}{n^2} (\bar{Y}_R - \bar{Y}_L)^2 \right) \\ = \frac{1}{n} \sum_{i \in P} (Y_i - \bar{Y})^2 - \frac{n_L n_R}{n^2} (\bar{Y}_R - \bar{Y}_L)^2, \end{aligned}$$

since  $n_L + n_R = n$ . Since the first term depends only on the parent node and not on the chosen split, we conclude that minimizing the CART criterion (1) is equivalent to maximizing the following expression

$$\frac{n_L n_R}{(n_L + n_R)^2} (\bar{Y}_L - \bar{Y}_R)^2. \quad (2)$$

This equivalent criterion can be interpreted as comparing the difference in the means of the resulting children nodes, i.e. we will choose the split such that the means in the children nodes is as heterogeneous as possible. The scaling factor  $\frac{n_L n_R}{(n_L + n_R)^2}$  appears naturally, penalizing uneven splits due to the increased variance of  $\bar{Y}_L$  or  $\bar{Y}_R$ .

### 2.3 Proof of Theorem 1

The first part of the Theorem is shown analogously to the proof in Section 2.2 of the supplement, but where we replace the standard dot product in  $\mathbb{R}$  with the inner product  $\langle \cdot, \cdot \rangle_{\mathcal{H}}$  associated with  $(\mathcal{H}, k)$  and use the induced RKHS norm  $\|\cdot\|_{\mathcal{H}}$ . Also, since  $k$  is bounded, the embedding  $\mu(\mathcal{D})$  into RKHS  $\mathcal{H}$  exists for any distribution  $\mathcal{D}$ , so everything is well-defined.

For the second statement of the Theorem 1, note that  $n_P \sim \text{Binomial}(p, n)$ , where  $\pi := \mathbb{P}(\mathbf{X} \in P) > 0$ . Let  $\hat{\mathbb{P}}(\mathbf{x}) = \hat{\mathbb{P}}(\mathbf{Y}|\mathbf{X} = \mathbf{x})$  be a fixed conditional distribution estimator and abbreviate for simplicity the true conditional distribution by  $\mathbb{P}(\mathbf{x}) = \mathbb{P}(\mathbf{Y}|\mathbf{X} = \mathbf{x})$ . We now write

$$\sum_{\mathbf{x}_i \in P} \left\| \mu(\delta_{\mathbf{y}_i}) - \mu(\hat{\mathbb{P}}(\mathbf{x}_i)) \right\|_{\mathcal{H}}^2 = \sum_{i=1}^n \left\| \mu(\delta_{\mathbf{y}_i}) - \mu(\hat{\mathbb{P}}(\mathbf{x}_i)) \right\|_{\mathcal{H}}^2 \mathbb{1}_{\{\mathbf{x}_i \in P\}}.$$

Then it holds that

$$\mathbb{E} \left[ \sum_{\mathbf{x}_i \in P} \left\| \mu(\delta_{\mathbf{Y}_i}) - \mu(\hat{\mathbb{P}}(\mathbf{X}_i)) \right\|_{\mathcal{H}}^2 \right] = n \mathbb{E} \left[ \mathbb{E} \left[ \left\| \mu(\delta_{\mathbf{Y}}) - \mu(\hat{\mathbb{P}}(\mathbf{X})) \right\|_{\mathcal{H}}^2 \middle| \mathbf{X} \right] \mathbb{1}_{\{\mathbf{X} \in P\}} \right]$$

and

$$\begin{aligned} \mathbb{E} \left[ \left\| \mu(\delta_{\mathbf{Y}}) - \mu(\hat{\mathbb{P}}(\mathbf{X})) \right\|_{\mathcal{H}}^2 \middle| \mathbf{X} \right] &= \mathbb{E} \left[ \mathbb{E} \left[ \left\| \mu(\delta_{\mathbf{Y}}) - \mu(\mathbb{P}(\mathbf{X})) \right\|_{\mathcal{H}}^2 \right] + \mathbb{E} \left[ \left\| \mu(\mathbb{P}(\mathbf{X})) - \mu(\hat{\mathbb{P}}(\mathbf{X})) \right\|_{\mathcal{H}}^2 \right] \middle| \mathbf{X} \right] \\ &\quad + 2 \mathbb{E} \left[ \langle \mu(\delta_{\mathbf{Y}}) - \mu(\mathbb{P}(\mathbf{X})), \mu(\mathbb{P}(\mathbf{X})) - \mu(\hat{\mathbb{P}}(\mathbf{X})) \rangle_{\mathcal{H}} \middle| \mathbf{X} \right]. \end{aligned}$$

Now for any  $f \in \mathcal{H}$ , we have:

$$\begin{aligned} \mathbb{E}[\langle \mu(\delta_{\mathbf{Y}}) - \mu(\mathbb{P}(\mathbf{X})), f \rangle_{\mathcal{H}} | \mathbf{X}] &= \mathbb{E}[\langle \mu(\delta_{\mathbf{Y}}), f \rangle_{\mathcal{H}} | \mathbf{X}] - \mathbb{E}[\langle \mu(\mathbb{P}(\mathbf{X})), f \rangle_{\mathcal{H}} | \mathbf{X}] \\ &= \mathbb{E}[f(\mathbf{Y}) | \mathbf{X}] - \mathbb{E}[\mathbb{E}[f(\mathbf{Y}) | \mathbf{X}] | \mathbf{X}] = 0, \end{aligned}$$

since from the definition of the embedding  $\mu$ , for  $\mathbf{Z} \sim \delta_{\mathbf{y}}$ , it holds

$$\langle \mu(\delta_{\mathbf{y}}), f \rangle_{\mathcal{H}} = \mathbb{E}[f(\mathbf{Z})] = f(\mathbf{y})$$

and for  $\mathbf{Z} \sim \mathbb{P}(\mathbf{x}) = \mathbb{P}(\mathbf{Y}|\mathbf{X} = \mathbf{x})$  we have

$$\langle \mu(\mathbb{P}(\mathbf{x})), f \rangle_{\mathcal{H}} = \mathbb{E}[f(\mathbf{Z})] = \mathbb{E}[f(\mathbf{Y}) | \mathbf{x}].$$

We finally conclude by taking  $f = \mu(\mathbb{P}(\mathbf{X})) - \mu(\hat{\mathbb{P}}(\mathbf{X})) \in \mathcal{H}$  that the cross term vanishes:

$$\mathbb{E} \left[ \langle \mu(\delta_{\mathbf{Y}}) - \mu(\mathbb{P}(\mathbf{X})), \mu(\mathbb{P}(\mathbf{X})) - \mu(\hat{\mathbb{P}}(\mathbf{X})) \rangle_{\mathcal{H}} \middle| \mathbf{X} \right] = 0$$

By using the general formula  $\mathbb{E}[g(\mathbf{X})|\mathbf{X} \in P] = \mathbb{E}[g(\mathbf{X})\mathbb{1}_{\{\mathbf{X} \in P\}}]/\mathbb{P}(\mathbf{X} \in P)$ , we finally obtain:

$$\begin{aligned}\mathbb{E}\left[\left\|\mu(\delta_{\mathbf{Y}}) - \mu(\hat{\mathbb{P}}(\mathbf{X}))\right\|_{\mathcal{H}}^2|\mathbf{X} \in P\right] &= \mathbb{E}\left[\left\|\mu(\delta_{\mathbf{Y}}) - \mu(\mathbb{P}(\mathbf{X}))\right\|_{\mathcal{H}}^2|\mathbf{X} \in P\right] + \mathbb{E}\left[\left\|\mu(\mathbb{P}(\mathbf{X})) - \mu(\hat{\mathbb{P}}(\mathbf{X}))\right\|_{\mathcal{H}}^2|\mathbf{X} \in P\right] \\ &= V(P) + \mathbb{E}\left[\left\|\mu(\mathbb{P}(\mathbf{X})) - \mu(\hat{\mathbb{P}}(\mathbf{X}))\right\|_{\mathcal{H}}^2|\mathbf{X} \in P\right]\end{aligned}$$

Define  $K = \sup_{z, z'} |k(z, z')| < \infty$ , as we have assumed that  $k$  is bounded. For any two distributions  $\mathcal{D}_1, \mathcal{D}_2$  we now obtain

$$\left\|\mu(\mathcal{D}_1) - \mu(\mathcal{D}_2)\right\|_{\mathcal{H}}^2 = \mathbb{E}[k(\mathbf{Z}_1, \mathbf{Z}'_1)] - 2\mathbb{E}[k(\mathbf{Z}_1, \mathbf{Z}_2)] + \mathbb{E}[k(\mathbf{Z}_2, \mathbf{Z}'_2)] \leq 4K,$$

where  $\mathbf{Z}_1, \mathbf{Z}'_1 \sim \mathcal{D}_1$  and  $\mathbf{Z}_2, \mathbf{Z}'_2 \sim \mathcal{D}_2$  are independent random variables. Thus,

$$\mathbb{E}\left[\left\|\mu(\delta_{\mathbf{Y}}) - \mu(\hat{\mathbb{P}}(\mathbf{X}))\right\|_{\mathcal{H}}^2\right] \leq 4K, \quad \mathbb{E}\left[\left\|\mu(\delta_{\mathbf{Y}}) - \mu(\hat{\mathbb{P}}(\mathbf{X}))\right\|_{\mathcal{H}}^4\right] \leq 16K^2$$

implying that both first and second moments of the random variable  $\left\|\mu(\delta_{\mathbf{Y}}) - \mu(\hat{\mathbb{P}}(\mathbf{X}))\right\|_{\mathcal{H}}^2 \mathbb{1}_{\{\mathbf{X} \in P\}}$  are finite. Moreover, since  $\left\|\mu(\delta_{\mathbf{y}_i}) - \mu(\hat{\mathbb{P}}(\mathbf{x}_i))\right\|_{\mathcal{H}}^2 \mathbb{1}_{\{\mathbf{x}_i \in P\}}$  for  $i = 1, \dots, n$  are its i.i.d. realizations, it follows directly from the CLT that:

$$\sqrt{n} \left( \frac{1}{n} \sum_{i=1}^n \left\|\mu(\delta_{\mathbf{y}_i}) - \mu(\hat{\mathbb{P}}(\mathbf{x}_i))\right\|_{\mathcal{H}}^2 \mathbb{1}_{\{\mathbf{x}_i \in P\}} - \pi \mathbb{E}\left[\left\|\mu(\delta_{\mathbf{Y}}) - \mu(\hat{\mathbb{P}}(\mathbf{X}))\right\|_{\mathcal{H}}^2|\mathbf{X} \in P\right] \right) = \mathcal{O}_p(1).$$

By multiplying the above equation with  $n/n_P = (1/\pi + o_p(1)) = \mathcal{O}_p(1)$ , it also holds that

$$\sqrt{n} \left( \frac{1}{n_P} \sum_{\mathbf{x}_i \in P} \left\|\mu(\delta_{\mathbf{y}_i}) - \mu(\hat{\mathbb{P}}(\mathbf{x}_i))\right\|_{\mathcal{H}}^2 - \frac{n\pi}{n_P} \mathbb{E}\left[\left\|\mu(\delta_{\mathbf{Y}}) - \mu(\hat{\mathbb{P}}(\mathbf{X}))\right\|_{\mathcal{H}}^2|\mathbf{X} \in P\right] \right) = \mathcal{O}_p(1),$$

Finally, by combining all the above results, we get the theorem statement:

$$\begin{aligned}&\sqrt{n} \left( \frac{1}{n_P} \sum_{\mathbf{x}_i \in P} \left\|\mu(\delta_{\mathbf{y}_i}) - \mu(\hat{\mathbb{P}}(\mathbf{x}_i))\right\|_{\mathcal{H}}^2 - \left( V(P) + \mathbb{E}\left[\left\|\mu(\mathbb{P}(\mathbf{X})) - \mu(\hat{\mathbb{P}}(\mathbf{X}))\right\|_{\mathcal{H}}^2|\mathbf{X} \in P\right] \right) \right) \\ &= \sqrt{n} \left( \frac{1}{n_P} \sum_{\mathbf{x}_i \in P} \left\|\mu(\delta_{\mathbf{y}_i}) - \mu(\hat{\mathbb{P}}(\mathbf{x}_i))\right\|_{\mathcal{H}}^2 - \mathbb{E}\left[\left\|\mu(\delta_{\mathbf{Y}}) - \mu(\hat{\mathbb{P}}(\mathbf{X}))\right\|_{\mathcal{H}}^2|\mathbf{X} \in P\right] \right) \\ &= \sqrt{n} \left( \frac{1}{n_P} \sum_{\mathbf{x}_i \in P} \left\|\mu(\delta_{\mathbf{y}_i}) - \mu(\hat{\mathbb{P}}(\mathbf{x}_i))\right\|_{\mathcal{H}}^2 - \frac{n\pi}{n_P} \mathbb{E}\left[\left\|\mu(\delta_{\mathbf{Y}}) - \mu(\hat{\mathbb{P}}(\mathbf{X}))\right\|_{\mathcal{H}}^2|\mathbf{X} \in P\right] \right) \\ &\quad - \sqrt{n} \left( 1 - \frac{n\pi}{n_P} \right) \mathbb{E}\left[\left\|\mu(\delta_{\mathbf{Y}}) - \mu(\hat{\mathbb{P}}(\mathbf{X}))\right\|_{\mathcal{H}}^2|\mathbf{X} \in P\right] = \mathcal{O}_p(1).\end{aligned}$$

The last equality holds since  $\mathbb{E}\left[\left\|\mu(\delta_{\mathbf{Y}}) - \mu(\hat{\mathbb{P}}(\mathbf{X}))\right\|_{\mathcal{H}}^2\right] \leq 4K$  and

$$\sqrt{n} \left( 1 - \frac{n\pi}{n_P} \right) = \mathcal{O}_p(1),$$

which in turn is true by another application of the CLT on random variables  $\mathbb{1}_{\{X_i \in P\}}$  and the fact that  $n/n_P = \mathcal{O}_p(1)$ :

$$\sqrt{n} \left( 1 - \frac{n\pi}{n_P} \right) = \sqrt{n} \frac{n_P - n\pi}{n_P} = \frac{n}{n_P} \frac{n_P - n\pi}{\sqrt{n}} = \mathcal{O}_p(1).$$

### 3 Simulation details

In this section we describe in detail all the simulations together with the data used in the analysis. The data sets are available in the R-package `drf` as well.



### 3.1 Air data

**Data.** This data is obtained from the website of the Environmental Protection Agency website ([https://aqs.epa.gov/aqsweb/airdata/download\\_files.html](https://aqs.epa.gov/aqsweb/airdata/download_files.html)). We have daily measurements for 5 years of data (2015-2019) for 6 'criteria' pollutants that form the Air Quality Index (AQI):

- O<sub>3</sub> - ground ozone (8 hours' average, expressed in pieces per million (ppm))
- SO<sub>2</sub> - sulfur dioxide (1 hour average, expressed in pieces per billion (ppb))
- CO - carbon monoxide (8 hours' average, expressed in pieces per million (ppm))
- NO<sub>2</sub> - nitrogen dioxide (1 hour average, expressed in pieces per billion (ppb))
- PM<sub>2.5</sub> - fine particulate matter smaller than 2.5 micrometers (24 hours' average, expressed in  $\mu g/m^3$ )
- PM<sub>10</sub> - large particulate matter, smaller than 10 micrometers (24 hours' average, expressed in  $\mu g/m^3$ )

For the above quantities, we have the maximal and mean value within the same day. In our analysis we have used only the maximal intraday values.

The pollutants are measured at different measurement sites. For each site we have information about

- site address (street, city, county, state, zip code)
- site coordinates (longitude and latitude)
- site elevation
- location setting (rural, urban, suburban)
- how the land is used within a 1/4 mile radius (agricultural, forest, desert, industrial, commercial, residential, blighted area, military reservation, mobile)
- date when the measurement site was put in operation
- date when the measurement site was decommissioned (NA if the site is still operational)

We have information about 19'739 sites, much more than the number of 2'419 sites from which we have measurements in years 2015-2019, since many sites were only operating in the past and are decommissioned.

In total there is 5'305'859 pollutant measurements. Many pollutants are measured at the same site, but it is important to note that not every site measures every pollutant, so there is a lot of 'missing' measurements. It can also occur that there are several measuring devices for the same pollutant at the same site, in which case we just average the measurements across the devices and do not report those measurements separately.

**Analysis.** Since we have a lot of missing data, we use only the data points (identified by the measurement date and the measurement site) where we have measurements of all the pollutants chosen as the responses. For that reason we also do not train DRF with all 6 pollutants as the responses, but only those that we are interested in, since only 64 sites measure all pollutants. For computational feasibility, we only use 50'000 of the available measurements for the training step. We also omit the states Alaska and Hawaii and the US territories for plotting purposes.

To obtain resultepts displayed in Figure 1, we train the DRF with the measurements (intraday maximum) of the two pollutants PM<sub>2.5</sub> and NO<sub>2</sub> as the responses, and the site longitude, latitude, elevation, land use and location settings as the predictors. We manually choose two decommissioned measurement sites (for which we have no measurements in years 2015-2019) as the test points. For each test point we obtain the weights to all training measurements. We further combine the weights for all measurements corresponding to the same site, which is displayed as the symbol size in the top row. The bottom row shows the estimated distribution of the response, where the transparency (alpha) each training point corresponds to the assigned weight. We also add some estimated contours.

For all plots in Figures 3 and 4, we train the single DRF with the same set of predictor variables and take the three pollutants O<sub>3</sub>, SO<sub>2</sub> and PM<sub>2.5</sub> as the responses. In this way we still have training data

from many different sites (see the above discussion on missing data) and moreover, those are the 3 pollutants that most likely cross the threshold for the "Good" AQI category set by the EPA. E.g. carbon monoxide (CO) almost never crosses this threshold.

In left plot of Figure 4, we compare the estimated CDF value with the classification forest which has a single response which is an indicator  $\mathbb{1}(\text{O}_3 < 0.055\text{ppm}, \text{SO}_2 < 36\text{ppb}, \text{PM}_{2.5} < 12.1\mu\text{g}/\text{m}^3)$ . In the right plot, we obtain the estimated CDF by fitting for each threshold a separate classification forest with an indicator  $\mathbb{1}(\text{O}_3 \leq \text{threshold})$ . We indeed pick a test point such that the classification performs bad, just to illustrate that its estimated CDF need not be monotone, which can not happen with DRF. In most of the cases, the estimated CDFs are very similar, as can also be seen from the left plot in Figure 4.

### 3.2 Benchmark analysis

In this part we compare the performance of DRF with several benchmark methods on a large number of data sets. Because our target of estimation is the whole conditional distribution and there is no canonical choice in the literature, one needs to use a special distributional loss. Furthermore, for any test point  $\mathbf{x}_i$  we only have one observation  $\mathbf{y}_i$  from  $\mathbb{P}(\mathbf{Y} | \mathbf{X} = \mathbf{x})$ , which makes performance evaluation of our estimator  $\hat{\mathbb{P}}(\mathbf{Y} | \mathbf{X} = \mathbf{x})$  very hard. We apply the following procedure: For a fixed conditional distribution estimator, we compute the induced distribution of the projected response  $\mathbf{w}^T \mathbf{Y}$  where the unit projection vector  $\mathbf{w}$  is sampled uniformly at random. We evaluate how well do we estimate the  $q = 0.9$  quantile by using the standard (univariate) quantile loss:

$$q \left( \mathbf{w}^T \mathbf{y}_i - \hat{Q}_{\mathbf{w}^T \mathbf{Y}}(\mathbf{x}_i) \right)_+ + (1 - q) \left( \hat{Q}_{\mathbf{w}^T \mathbf{Y}}(\mathbf{x}_i) - \mathbf{w}^T \mathbf{y}_i \right)_+$$

For a given data set, we apply 2-fold cross validation to compute the average quantile loss for a given  $\mathbf{w}$  and report the average rank of each method over 100 random draws of  $\mathbf{w}$ .

We also preprocess each data set by performing local centering [?], where we subtract the marginal conditional means. Estimating the marginal means can be done straightforwardly by using univariate regression, but here we want to investigate how well one can detect also the interactions between different components of  $\mathbf{Y}$ . Furthermore, many data sets used have relatively small sample size for such a complicated task of estimating the full conditional distribution, thus favoring methods which just consider the marginal means.

#### Competing methods

We compare two versions of DRF (using the CART or the MMD splitting criterion) with several straightforward methods that can be used for estimation of the conditional distribution.

- **k-NN:** The standard k-nearest neighbors algorithm with the Euclidean metric. An estimated conditional distribution  $\hat{\mathbb{P}}(\mathbf{Y} | \mathbf{X} = \mathbf{x})$  at a test point  $\mathbf{x}$  is defined by a uniform distribution on the  $k$  nearest observations in the training set.  $k$  is chosen for each data set by using 10-fold cross-validation from a prespecified grid.
- **Gaussian kernel:** The estimate of the conditional distribution  $\hat{\mathbb{P}}(\mathbf{Y} | \mathbf{X} = \mathbf{x})$  at a test point  $\mathbf{x}$  is obtained by assigning to each training observation  $(\mathbf{x}_i, \mathbf{y}_i)$  the weight proportional to the Gaussian kernel  $k(\mathbf{x}, \mathbf{x}_i)$ , analogously to usual kernel estimation methods.
- **Homogeneous distribution model:** The estimated conditional distribution  $\hat{\mathbb{P}}(\mathbf{Y} | \mathbf{X} = \mathbf{x})$  is obtained by assigning the same weight to every training point. In combination with local centering, this method makes the homogeneity assumption that the residuals have constant distribution and only the conditional mean change.

#### Benchmark datasets

Many benchmark data sets used come from the multiple target regression literature, where only the conditional means of the multivariate response is considered. We have used the data sets: **jura**, **slump**, **wq**, **enb**, **atp1d**, **atp7d**, **scpf**, **sf1** and **sf2** collected in the Mulaan [?] library. Description about the dimensionality of the datasets, together with the descriptions of the outcomes and the regressors can be found in [?] with links to the relevant papers introducing these datasets. In each data

set categorical variables have been represented by the one-hot dummy encoding, the observations with missing data were removed together with constant regressors.

We additionally added 4 data sets obtained from different applications in this paper:

- **copula**: Simulated Gaussian copula example in the paper.
- **birth1**: This data set is created from the CDC natality data and contains many covariates as predictors and the pregnancy length and birthweights as the responses.
- **birth2**: This data set is similar as the above one, but we take pregnancy length as the predictor and add 3 more measures of baby's health as the response: APGAR score measured 5 minutes after birth and indicators whether there were any abnormal conditions and congenital anomalies.
- **wage**: This data set is created from the 2018 American Community Survey. We take the logarithmic hourly wage and gender as the response, as it was done in the fairness example in the main paper.
- **air**: This data set is obtained from the EPA air quality data. All six pollutants were taken as the response and we add both the information about the measuring site (location, which setting it is in, etc.), as well as the temporal information when the measurement has taken place (month, day of the week).

### 3.3 Birth data

**Data.** This data set is obtained from the CDC Vital Statistics Data Online Portal ([https://www.cdc.gov/nchs/data\\_access/vitalstatsonline.htm](https://www.cdc.gov/nchs/data_access/vitalstatsonline.htm)) and contains the information about the  $\approx 3.8$  million births in 2018. However, as we do not need this many data points, we subsample 300'000 of them. Even though the original data contains a lot of variables, we have taken only the following variables from the source data:

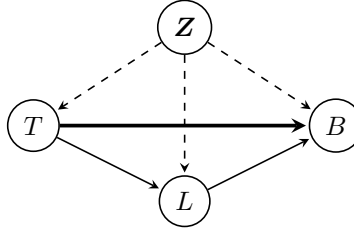
- mother's age, height, weight before the pregnancy and BMI before pregnancy
- mother's race (black, white, asian, NHOPI, AIAN or mixed), marital status (married or unmarried) and the level of education (in total 8 levels)
- father's age, race and education level
- month and year of birth
- plurality of the birth (how many babies were born at once)
- Whether and when the prenatal care started
- length of the pregnancy
- delivery method (vaginal or C-section)
- birth order - the total number of babies born by the same mother (including the current one)
- birth interval - number of months passed since last birth (NA if this is the first child)
- number of cigarettes smoked per day on average during the pregnancy
- birthweight (in grams) and gender of the baby
- APGAR score (taken after 5min and 10min)
- indicators whether baby had any abnormal condition or some congenital anomalies

**Analysis.** After removing the data points with any missing entries and taking only the data points where the race of both parents is either black, white or Asian (for nicer plotting), we are left with 183'881 data points. We use randomly chosen 100'000 data points for training the DRF. We take the birthweight and the pregnancy length as the bivariate response and for the predictors we take: mother's age, race, education, marital status, height, BMI; father's age, race and education level; birth plurality, birth order, delivery method, baby's gender, number of cigarettes and indicator whether prenatal care took place.

For arbitrary test points from the data we can get the estimated weights by the fitted DRF, thus estimating the joint distribution of birthweight and pregnancy length conditional on all other variables mentioned above. Two such distributions are shown in Figure 6. In addition we use the weights to fit a parametric model for the mean and 0.1 and 0.9 quantiles. This is done as follows:

- We slightly upweight the data points where the pregnancy length is significantly above or below the usual range. This is to avoid the bulk of the data points to dominate the fit obtained for very long or short pregnancies.
- We apply the transformation  $f(\cdot) = \log(\log(\cdot))$  on both the pregnancy length and the birthweight since then the scatterplots look much nicer.
- We estimate the mean with smoothing splines with a small manually chosen number of degrees of freedom.
- The fitted mean is subtracted from the response (birthweight). The residuals seem well behaved with maybe slight, seemingly linear trend in standard deviation.
- We fit the 0.1 and 0.9 quantiles as the best linear functions that minimize the sum of quantile losses, by using the `quantreg` package [?].
- The data is transformed back on the original scale by using the function  $f^{-1}(\cdot) = \exp(\exp(\cdot))$ .

For the right plot in Figure 6, we have the following causal graph:



We want to determine the direct effect (indicated in bold) of the twin pregnancy  $T$  on the birthweight  $B$  that is due to sharing of resources by the babies (space, food etc.) and is not due to the fact that twin pregnancy causes shorter pregnancy length  $L$ , which in turn causes the smaller birthweight. Another big issue is that we have confounding factors  $Z$  which can directly affect  $B$ ,  $L$  and  $T$ . For example, the number of twin pregnancies significantly depends on the parents' race, but so do the pregnancy length and the birthweight, e.g. black people have more twins, shorter pregnancies and smaller babies. We take all other variables as the potential confounders  $Z$  and adjust for all of them (mother's age, race, education, marital status, height, BMI; father's age, race and education level; birth plurality, birth order, baby's gender, number of cigarettes and indicator whether prenatal care took place). In order to do it, we fit the same DRF as before, where  $Z$  and  $T$  are the predictors and  $(B, L)$  is the bivariate response for which we can nicely fit the parametric model described above. We compute then the interventional distribution  $\mathbb{P}(B \mid do(T = t, L = l))$  for all values of  $t$  and  $l$ , by using the do-calculus to adjust the confounding  $Z$  via the backdoor criterion [?], where we also use the obtained parametric regression fit. In this way we can generalize the fit well, which is important when doing the do-calculus, since we are interested in some hypothetical combinations of covariates which might not occur frequently in the observed data, such as very long twin pregnancies.

### 3.4 Wage data

**Data.** The PUMS (Public Use Microdata Area) data from the 2018 1-Year American Community Survey is obtained from the US Census Bureau API (<https://www.census.gov/content/dam/Census/data/developers/api-user-guide/api-guide.pdf>). The survey is sent to  $\approx 3.5$  million people annually and aims to give more up to date data than the official census that is carried out every decade. The 2018 dataset has 3'214'539 anonymized data points for the 51 states and District of Columbia. Even though the original survey contains many questions, we have retrieved only the subset of variables that might be relevant for the salaries:

- person's gender, age, race (AIAN, black, white, asian, mix, NHOPI, other), indicator of hispanic origin, state of residence, US citizenship indicator (5 ordered levels), indicator whether the person is foreign-born
- person's marital status, number of own children in the same household and the number of family members in the same household

- person's education level (24 ordered levels) and level of English knowledge (5 ordered levels)
- person's employment status (employed, not at work, not in workforce, unemployed)
- for employed people we have annual salary earnings, number of weeks worked in a year and average number of hours worked per week
- for employed people we have employer type (government, non-profit company, for-profit company, self-employed), occupation (530 levels), industry where the person works (271 levels) and the geographical unit where the person works (59 levels)
- statistical weight determined by the US Census Bureau which aims to correct sampling bias

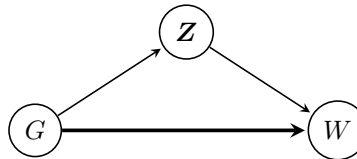
For our purposes, since we want to analyze the unfairness of the gender pay gap, we consider only employed people that are at least 17 years of age, have worked full-time (at least 48 weeks in a year) and have worked at least 16 hours a week on average. We also omit the self-employed persons, since they often report zero annual salary and the pay gap there, if exists, can not be called unfair as the salary is not determined by any employer. Since there are no missing data which would need to be omitted, we finally end up with 1'071'866 data points.

**Analysis.** We scale the salary with the amount of time spent working (determined from the number of weeks worked and average hours worked per week) to compute the logarithm of the hourly wages. The scaling with the time spent working is necessary, since full-time employed men spend on average 11% more time working than women. The logarithmic transformation is used since the salaries are very skewed (positively) and logarithmic wages show nice behavior.

We also reduce the large number of levels of some of the categorical variables: for the occupation we use the group of 530 jobs into 20 categories provided in the SOC system (<https://www.bls.gov/soc/>); for the industry information we group the 271 possibilities in 23 categories as is done in the NIACS classification (<https://www.bls.gov/bls/naics.htm>); for the work place we group the 59 US states and foreign territories into 9 economic regions (including the "abroad" category), as determined by the Bureau of the Economic Analysis (<https://apps.bea.gov/regional/docs/regions.cfm>).

We want to investigate how is the logarithmic hourly wage  $W$  affected by the gender  $G$ , depending on the other factors  $\mathbf{Z}$ : age, race, hispanic origin, citizenship, being foreign-born, marital status, family size, number of children, education level, knowledge of English, occupation, industry type and place of work. To do this, we train DRF with bivariate response  $(W, G)$  and predictors  $\mathbf{Z}$  on a subsample of 300'000 data points. With it we can answer for fixed values of covariates  $\mathbf{Z} = \mathbf{z}$ , what are distribution of salaries of men and women. In addition, we can determine the "propensities", i.e. the proportion of men and women corresponding to  $\mathbf{Z} = \mathbf{z}$ . This information is displayed in the left plot of Figure 7 for a combination of covariates corresponding to some person in the left-out data. Three additional such plots can be seen in the Figure 1 (of this document), illustrating how the distribution of salaries and their relationship can vary with different covariates  $\mathbf{Z}$ .

We do not only want to determine how different covariates  $\mathbf{Z}$  affect the salary distribution, but we want to quantify the overall fairness of the pay, after appropriate adjustments. In the Figure 1 of this document, we can see that the observed salaries of men and women differ noticeably, and this difference in the logarithmic wages means that an average woman has 16% smaller salary than an average men. However, the question is how much of this difference is "fair". For example, the effect of the gender on the salary can be mediated through some variables such as, for example, the occupation, workplace or the level of education and we are only interested in the direct effect. This is illustrated in the following causal graph:



If we assume that people have the freedom to choose such variables themselves, the pay gap which arises from such different choices for men and women is fair and those variables are resolving

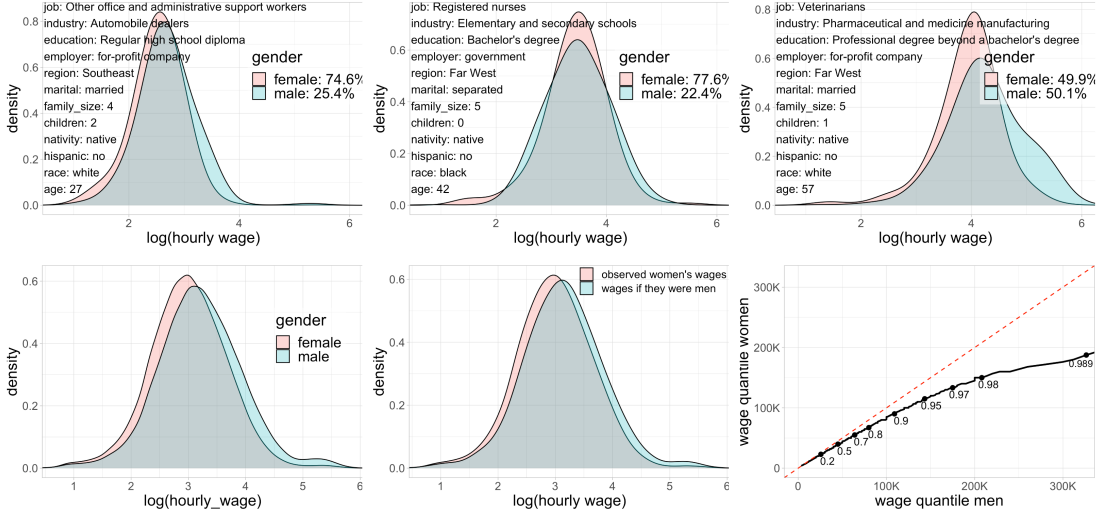


Figure 1: Top row: the estimated conditional distributions  $\mathbb{P}(W, G | \mathbf{Z} = \mathbf{z})$ , for different values of the covariates  $\mathbf{z}$  as indicated in the plots. Bottom row: observed distribution of men's and women's wage (left); the comparison of the distributions of the observed women's wages and the counterfactual wages had the women been men, while keeping the same characteristics  $\mathbf{Z}$  (middle) and comparison of the corresponding quantiles of those two distributions (right).

variables [?]. Another way that the pay gap can be explained is that some of the variables are not statistically independent of the gender in the population of full-time employed people (e.g. the race or the age), but they themselves have an effect on the salary.

In order to address those issues, we compute the distribution of the nested counterfactual  $W(\text{male}, \mathbf{Z}(\text{female}))$ , corresponding to the wages of a person that has characteristics  $\mathbf{Z}$  as a woman, but which was treated as a man for obtaining the salary. Such distribution can be computed from the DRF, as described in the main paper: we randomly draw a female person and for its characteristics  $\mathbf{z}$  we obtain the conditional distribution of wages of men with those characteristics  $\mathbb{P}(W | G = \text{male}, \mathbf{Z} = \mathbf{z})$  via the weights. Those distributions are averaged over random draw of 1'000 women (that were not used in the training step of the DRF). In case that the difference in salary is fair, the distribution of the counterfactual salary  $W(\text{male}, \mathbf{Z}(\text{female}))$  should be exactly the same as the observed distribution of women's wages. However, we can see that this is not the case and that the medians salaries of the two distributions differ by 14%. Even though this is smaller than the 16% we obtain by comparing only the observational distributions, it still shows that the women are paid less compared to men.